International Conference on Applied Energy 2019
Aug 12-15, 2019, Västerås, Sweden
Paper ID: 1049

TEMPORAL COMPLEMENTARITY BETWEEN THREE VARIABLE RENEWABLE ENERGY SOURCES: A SPATIAL REPRESENTATION

Fausto A. Canales[1*], Jakub Jurasz[2,3], Alexander Kies[4], Alexandre Beluco [5], Marco Arrieta-Castro[1], Andrés Peralta-Cayón[1]

1 Department of Civil and Environmental, Universidad de la Costa, Calle 58 #55-66, 080002 Barranquilla, Atlántico, Colombia.
*fausto.canales.v@gmail.com (Corresponding Author)

2 MDH University, School of Business Society and Engineering, Högskoleplan 1, 722 20 Västerås, Sweden

3 AGH University, Faculty of Management, Department of Engineering Management, 30 Mickiewicza Ave., 30-059 Kraków, Poland

4 Frankfurt Institute for Advanced Studies, Goethe University Frankfurt, Ruth-Moufang-Str. 1, 60438 Frankfurt am Main, Germany

5 Instituto de Pesquisas Hidráulicas, Universidade Federal do Rio Grande do Sul, Av Bento Goncalves, 9500, Porto Alegre, RS, Brazil

ABSTRACT

This paper presents a method for spatially representing the total temporal energetic complementarity between three different variable renewable sources, by means of an index created from correlation coefficients and compromise programming. The method is employed to study the complementarity of wind speed, solar radiation and surface runoff on a monthly scale using continental Colombia as case study, during the year of 2015. Results show that the combination of solar radiation and surface runoff presented the highest energetic complementarity during this year, heavily influenced by El Niño phenomenon.

Keywords: energetic complementarity, renewable energy, variable renewables, correlation, compromise programming, geographic information systems

NOMENCLATURE

Abbreviations	
GIS	Geographic Information Systems
VRES	Variable Renewable Energy Sources
Symbols	
κ_t	total temporal complementarity index

1. INTRODUCTION

One of the main concerns related to some renewables is their usually common variability, produced by meteorological factors. This features frequently poses a challenge for integrating these energies into national power grids [1], and constitutes one of the main drawbacks of stand-alone systems based on variable renewable energy sources (VRES), because it might result in performance issues or system oversizing [2].

One option to overcome this shortcoming is to consider hybrid power systems integrating two or more VRES in a combination in which these sources complement each other. This energetic complementarity is usually expressed in terms of a correlation coefficient or complementarity index. Both types of metrics are used to describe the potential of energy sources to complement each other on a temporal, spatial or spatiotemporal scale, thereby ensuring supply reliability and minimizing power output fluctuations or shortages. The spatial representation of energetic complementarity has been conducted by some authors like Silva et al. [3], Cantão et al. [4], Vega-Sánchez et al. [5] and Risso et al. [6]. The paper by Borba and Brito [7] was the only paper found that presents a spatial representation of a metric assessing complementarity between more than three sources, extending from the method for estimating a complementarity index, developed by Beluco [8].

From the above observations, this paper presents a method for the spatial representation of an index describing the temporal energetic complementarity between three VRES. The method is an extension from the manuscript by Canales et al. [9], which is based on linear metric built on correlation coefficients and compromise programming. The continental territory of Colombia was used as case study for this paper.

2. MATERIAL AND METHODS

The method presented in this paper is based on the work by Canales et al. [9], extending it in order to perform a spatial evaluation and comparison of temporal energetic complementarity between pairs of resources and a joint combination of three VRES.

This section also summarizes the main inputs used in a case study for illustrating the method described.

2.1 Method

Correlation metrics allow assessing at which level two variables are linearly related. From the perspective of VRES, correlation coefficients can be used to assess if one resource is able to supplement or complement the energy production capacity of another. Negative correlation coefficients between a pair of VRES indicate some degree of temporal energetic complementary [10]. Based on Cantão et al. [4], Table 1 describes the adopted interpretation of the correlation coefficient value. For this paper, authors use Pearson's as the correlation type, resulting in three different values of $f_k(\mathbf{c})$, one for each paired combination of resources.

Table 1 Correlation coeff. interpretation (Adapted from [4]).

Correlation coefficient (CC) values	Interpretation
0.9 ≤ CC ≤ 1.0	Very strong similarity
0.6 ≤ CC < 0.9	Strong similarity
0.3 ≤ CC < 0.6	Moderate similarity
0.0 ≤ CC < 0.3	Weak similarity
-0.3 < CC ≤ 0.0	Weak complementarity
-0.6 < CC ≤ -0.3	Moderate complementarity
-0.9 < CC ≤ -0.6	Strong complementarity
-1.0 ≤ CC ≤ -0.9	Very strong complementarity

For allowing the assessment of the joint complementarity between the 3 VRES, one suitable method is the utilization of multi-criteria analysis techniques, with compromise programming being the method chosen for this paper. This technique focuses on finding the closest point to the ideal solution, within the domain of the feasible solutions. According to Gershon and Duckstein [11] equation 1 can be used for calculating the metric Lp, that in compromise programming represents the distance of each option $f_k(\mathbf{c})$ to the optimal solution (usually unfeasible):

$$L_p(\boldsymbol{c}) = \left[\sum_{k=1}^{n} \alpha_k^p \left|\frac{f_k^{best} - f_k(\boldsymbol{c})}{f_k^{best} - f_k^{worst}}\right|^p\right]^{1/p} \tag{1}$$

where: α_k^p are the weights for each component k (where k is each paired combination). As described in [9], the method considers that all paired combinations have the same importance, therefore, $\alpha_k^p = 1$ for all cases. Also in equation (3), $f_k(\mathbf{c})$ is the correlation coefficient for the corresponding paired combination of resources; f_k^{best} is the most desirable value of the correlation functions, therefore, $f_k^{best} = -1$, because it would represent full complementarity; f_k^{worst} is the less desirable value of the correlation functions, then, $f_k^{worst} = 1$, because it would represent full similarity (i.e., the simultaneous occurrence); p is the parameter that defines the type of geometrical distance between f_k^{best} and $f_k(\mathbf{c})$. When p = 1 (as in this paper), Gershon and Duckstein [11] explain that all deviations from f_k^{best} are considered in direct proportion to their magnitudes. For 2 (Euclidean distance) ≤ p < ∞, the largest deviation has the greatest influence.

When considering three sources, the total temporal complementarity index κ_t can be calculated by normalizing the *Lp(c)* metric through the following expression:

$$\kappa_t(\boldsymbol{c}) = \frac{3 - Lp(\boldsymbol{c})}{2.25} \tag{2}$$

with κt values ranging from 0 (perfect synchronicity between the three VRES) to 1 (perfect complementarity). Values closer to 1 would indicate a more uniform aggregate behavior of the three time-series, while values closer to 1 would present greater amplitudes in terms of peaks and valleys of this aggregate behavior. A general demonstration of how equation (2) was derived can be found in the appendix section of Canales et al. [9]. The process for creating the energetic complementarity map between the 3 VRES is summarized in Fig 1.

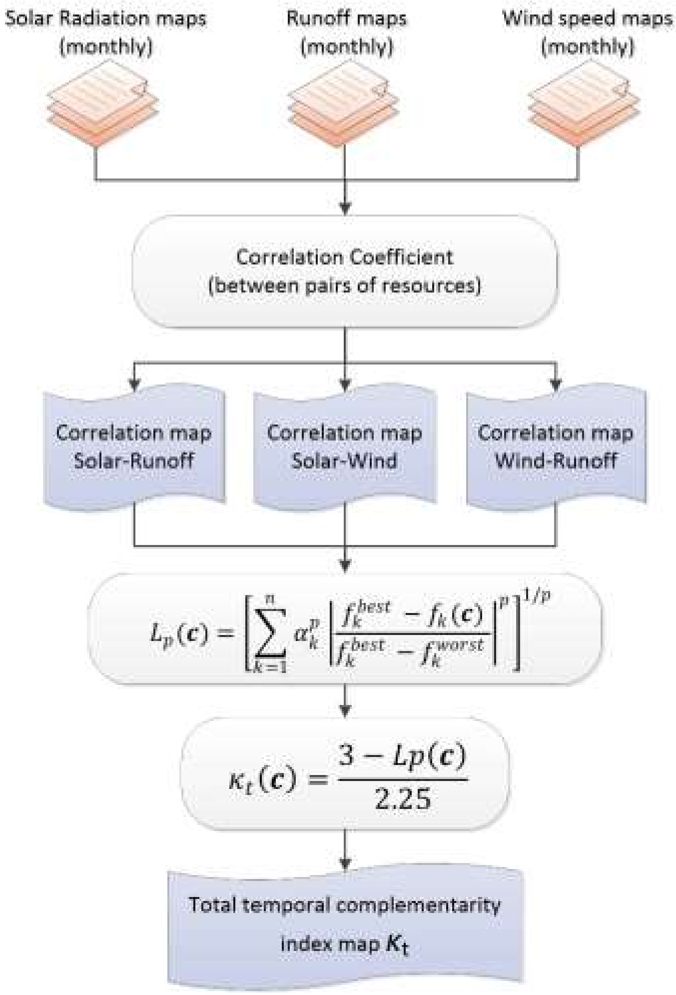

Fig 1 Diagram describing the method for the spatial representation of complementarity between 3 VRES

2.2 Case study

Situated at the northern part of South America, the continental territory of Colombia was used as case study (approx. 1,142,748 km^2) for this paper. The dataset used in this work corresponds to the average monthly solar net radiation, surface runoff and wind speed at 10 m from ERA5 reanalysis [12] for the year of 2015. The intensity of El Niño phenomenon was particularly strong that year [13], with anomalously warm sea surface temperatures that suggest that a 100% natural origin is unlikely [14].

3. RESULTS AND DISCUSSION

This section succinctly presents the main findings of this study. Using the data and methods described in the previous section, Fig 2 to Fig 4 present the correlation for each paired combination of resources, as well as their corresponding percentages for each classification defined at Table 1.

The results shown in Fig 2 indicate most of the country presents a complementary behavior between solar radiation and surface runoff. However, it must be pointed out that this does not automatically mean that hydropower potential is available at all regions, because this generation capability is also defined by available head and the main courses of rivers, and both features depend on favorable and specific terrain features.

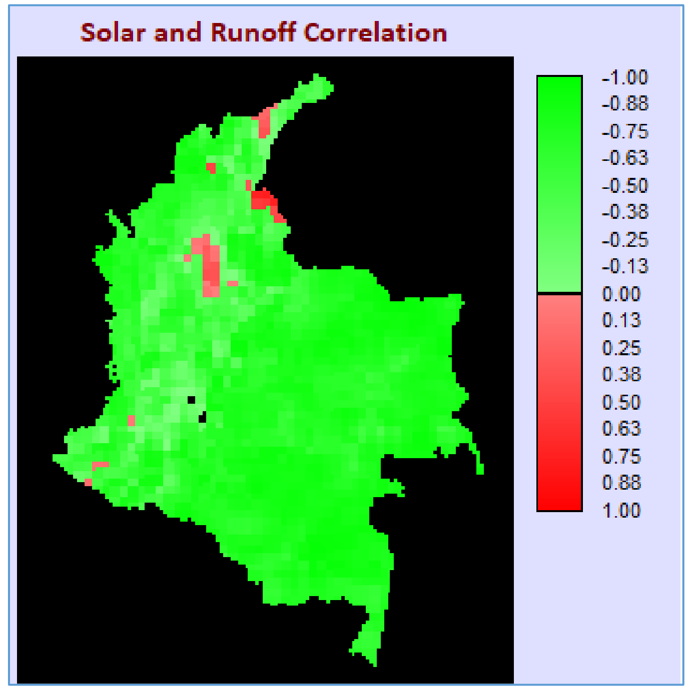

Fig 2 Correlation map for radiation and surface runoff

The wind speed and solar radiation correlation map (Fig 3) show that most of the territory exhibits a similar behavior between these two VRES, except for some regions, specifically near Darien, Amazonia and the mountain chains (Cordillera Oriental and Cordillera Central).

Similar to solar radiation and surface runoff, most of the country presents a complementary behavior along the year for wind speed and surface runoff (Fig 4).

As previously mentioned in this document, the year in analysis was marked by el Niño phenomenon, which usually brings droughts and forest fires within Colombia. Besides the low precipitation and corresponding surface runoff, the high similarity between wind and solar resources during this year could be explained by the relation between these two resources. Wind is an indirect form of solar energy, and is caused by differential heating of the earth's surface by the sun [15].

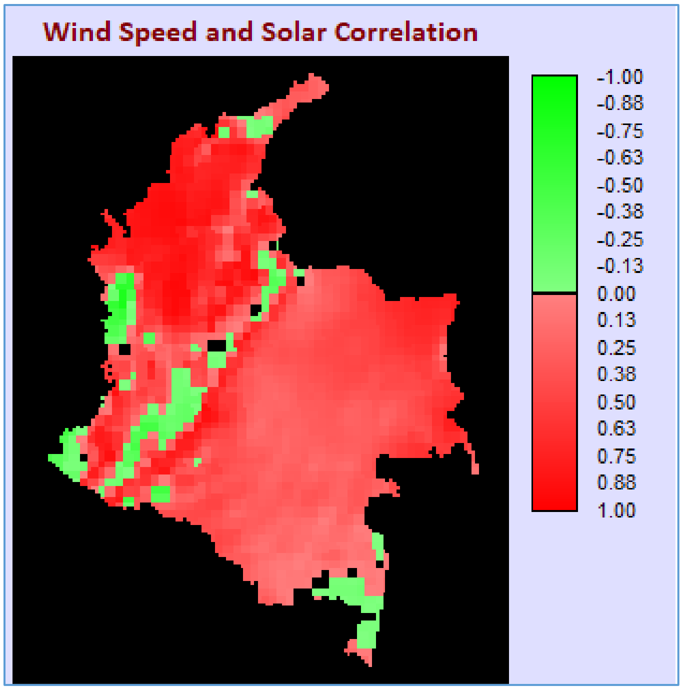

Fig 3 Correlation map for radiation and wind speed

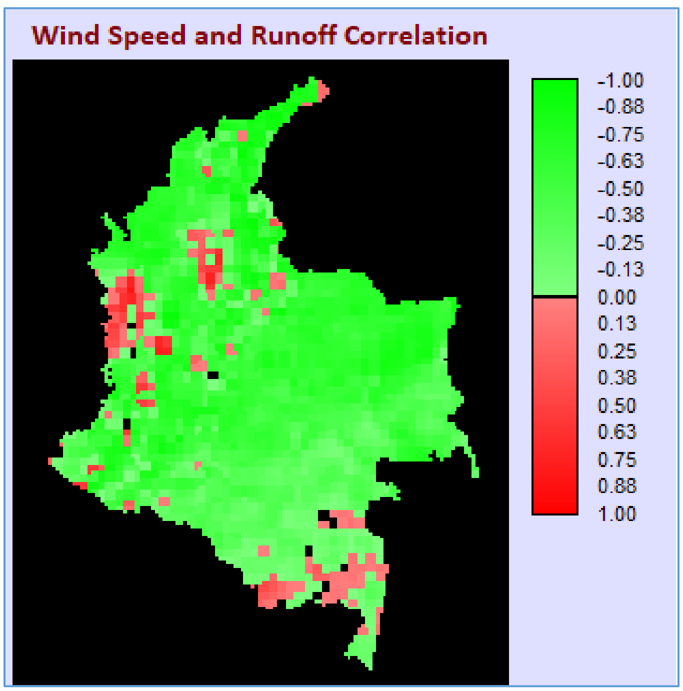

Fig 4 Correlation map for surface runoff and wind speed

Once the three correlation maps are found, the process described in Fig 1 is applied, resulting in the map shown in Fig 5, which presents the κt values for the entire territory under consideration. Normalizing the correlation values within a scale from 0 (full similarity) to 1 (full complementarity) allows estimating which one of the four possible combinations presented from Fig 2 to Fig 5 is the best option at each location.

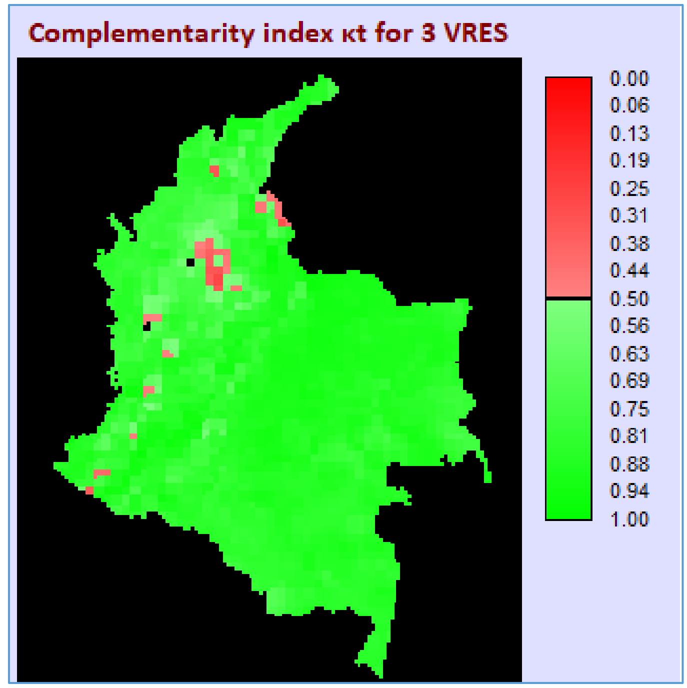

Fig 5 Map showing KT index at each location

These results from the aforementioned normalization are shown in Fig 6, with results suggesting that, in terms of complementarity, the higher normalized score for most of the country is obtained from the correlation between radiation and runoff, followed by the complementarity between the 3 VRES. These results could be used as a starting point for regional planning related to hybrid power systems and the method can be easily applied to other areas of the world and to other VRES like biomass and from the ocean.

4. CONCLUSIONS

This paper described a method for the spatial representation of the temporal complementarity between three VRES: solar radiation, surface runoff and wind speed. The monthly averages for these resources were obtained from ERA5 reanalysis [12] for the year of 2015, using the continental territory of Colombia as case study. For this year influenced by El Niño phenomenon, the combination of solar radiation and surface runoff presented the highest energetic complementarity.

The method could be applied to other regions of the world, and its results might help in the initial assessments for regional planning of hybrid power systems based on VRES. Extended works could evaluate the impact of different climate conditions and time scales.

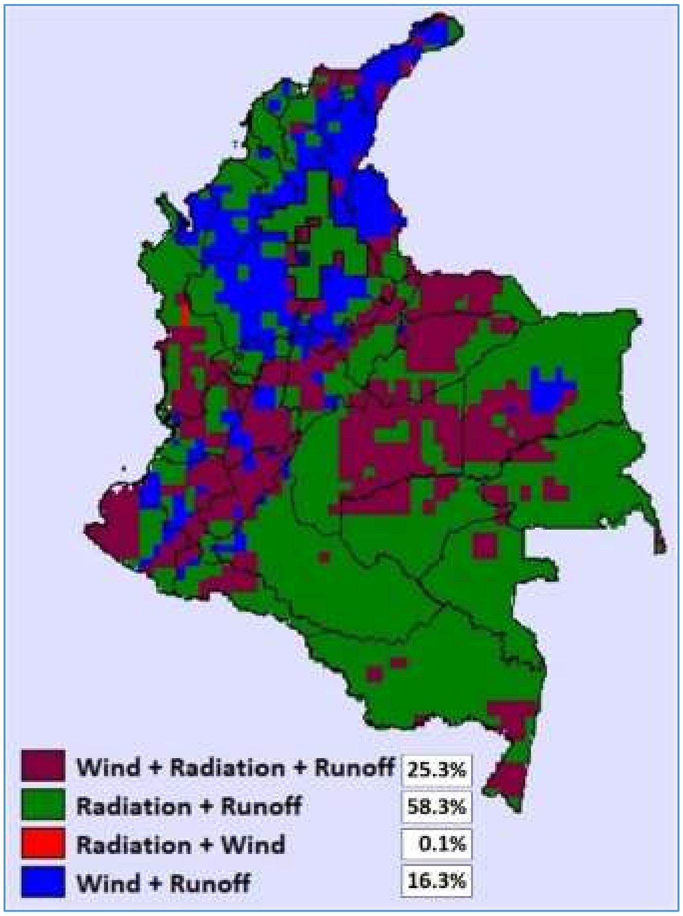

Fig 6 Map of best options in terms of complementarity

ACKNOWLEDGEMENTS

The authors are grateful for the support received by their institutions for the research work that resulted in this paper. The fourth author acknowledges the financial support received from CNPq for his research work (proc. n.312941/2017-0).

REFERENCES

[1] Ming B, Liu P, Guo S, Zhang X, Feng M, Wang X. Optimizing utility-scale photovoltaic power generation for integration into a hydropower reservoir by incorporating long- and short-term operational decisions. Appl Energy 2017;204:432–45. doi:10.1016/j.apenergy.2017.07.046.

[2] Safaei H, Keith DW. How much bulk energy storage is needed to decarbonize electricity? Energy Environ Sci 2015;8:3409–17. doi:10.1039/c5ee01452b.

[3] Silva AR, Pimenta FM, Assireu AT, Spyrides MHC. Complementarity of Brazil ' s hydro and offshore wind power. Renew Sustain Energy Rev 2016;56:413–27. doi:10.1016/j.rser.2015.11.045.

[4] Cantão MP, Bessa MR, Bettega R, Detzel DHM, Lima JM. Evaluation of hydro-wind complementarity in the Brazilian territory by means of correlation maps. Renew Energy 2017;101:1215–25. doi:10.1016/j.renene.2016.10.012.

[5] Vega-Sánchez MA, Castañeda-Jiménez PD, Peña-Gallardo R, Ruiz-Alonso A, Morales-Saldaña JA, Palacios-hernández ER. Evaluation of Complementarity of Wind and Solar Energy Resources over Mexico using an Image Processing Approach. IEEE Int. Autumn Meet. Power, Electron. Comput., Ixtapa, Mexico Evaluation: IEEE; 2017, p. 1–5.

[6] Risso A, Beluco A, De Cássia Marques Alves R. Complementarity roses evaluating spatial complementarity in time between energy resources. Energies 2018;11:1–14. doi:10.3390/en11071918.

[7] Borba EM, Brito RM. An Index Assessing the Energetic Complementarity in Time between More than Two Energy Resources. Energy Power Eng 2017;09:505–14. doi:10.4236/epe.2017.99035.

[8] Beluco A, de Souza PK, Krenzinger A. A dimensionless index evaluating the time complementarity between solar and hydraulic energies. Renew Energy 2008;33:2157–65. doi:10.1016/j.renene.2008.01.019.

[9] Canales FA, Jurasz J, Beluco A, Kies A. Assessing temporal complementarity between three variable energy sources by means of correlation and compromise programming. ArXiv: 190500117 [PhysicsSoc-Ph] 2019.

[10] Slusarewicz JH, Cohan DS. Assessing solar and wind complementarity in Texas. Renewables Wind Water, Sol 2018;5:7. doi:10.1186/s40807-018-0054-3.

[11] Gershon M, Duckstein L. Multiobjective Approaches to River Basin Planning. J Water Resour Plan Manag 1983;109:13–28. doi:10.1061/(ASCE)0733-9496(1983)109:1(13).

[12] Copernicus Climate Change Service (C3S). ERA5: Fifth generation of ECMWF atmospheric reanalyses of the global climate . Copernicus Climate Change Service Climate Data Store (CDS) 2017. https://cds.climate.copernicus.eu/cdsapp#!/home (accessed April 28, 2019).

[13] Centro de Previsão de Tempo e Estudos Climáticos / Instituto Nacional de Pesquisas Espaciais. El Niño e La Niña 2016. http://enos.cptec.inpe.br/ (accessed May 5, 2019).
[14] Newman M, Wittenberg AT, Cheng L, Compo GP, Smith CA. The Extreme 2015/16 El Niño, in the Context of Historical Climate Variability and Change. Bull Am Meteorol Soc 2018;99:S16–20. doi:10.1175/BAMS-D-17-0116.1.
[15] Joselin Herbert GM, Iniyan S, Sreevalsan E, Rajapandian S. A review of wind energy technologies. Renew Sustain Energy Rev 2007;11:1117–45. doi:10.1016/j.rser.2005.08.004.